Inhomogeneous broadening of energy levels due to fluctuations of doping concentration in quantum-cascade lasers

© An.A. Afonenko¹, A.A. Afonenko¹, D.V. Ushakov¹, R.A. Khabibullin²

220030 Minsk, Republic of Belarus

² National Research Center "Kurchatov Institute",

117105 Moscow, Russia

E-mail: afonenko@bsu.by Received March 26, 2025 Revised June 23, 2025 Accepted June 23, 2025

The influence of fluctuations of the concentration of charged impurities on the current-voltage characteristics of quantum-cascade lasers at the coherence length of electron wave functions exceeding the screening length of the Coulomb potential is analyzed. It is found that the value of inhomogeneous broadening of the transition lines can exceed the values for the homogeneous broadening for the corresponding levels. The value of inhomogeneous broadening appears to be larger for the wave functions, which are more separated in space.

Keywords: quantum-cascade heterostructures, ionized impurities, inhomogeneous spectral broadening.

DOI: 10.61011/SC.2025.02.61363.7737

1. Introduction

Quantum cascade lasers (QCL) based on interband electron transitions are compact, efficient semiconductor radiation sources in the mid-IR and terahertz ranges. The highest operating temperatures achieved in the terahertz frequency range (~4 THz) are 261 K with pulsed pumping [1]. The QCL radiation power in the frequency range of 3 THz reaches 230 mW in continuous operation [2] and several watts in pulse mode [3]. An important step in the creation of lasers is numerical modeling and optimization of characteristics. Modeling of the terahertz frequency range by the method of balanced equations based on the basis of wave functions with reduced dipole moments of tunnel-coupled states [4] demonstrated its effectiveness in the manufacture of the first samples by molecular beam epitaxy [5], allowed selecting a design suitable for growing by the method of metal-organic vapor deposition [6], as well as the efficient two-photon design [7], which demonstrates record-low threshold current densities ($\sim 100 \, \text{A/cm}^2$) in continuous operation [8]. The improvement of theoretical QCL models continues to be an urgent task, since a complete quantitative correspondence of the calculated and experimental results has not yet been achieved.

Combinations of eigenstates with close energies are chosen as the basis in the balanced equation method in Ref. [4], so that the length of the wave functions decreases in the direction of the normal to the plane of the layers. At the same time, the overlap of the wave functions decreases and, accordingly, the total probability of transitions decreases, although the off-diagonal matrix elements of the Hamiltonian additionally lead to tunneling processes. The purpose of this study is to analyze the effect

of electron localization in the plane of the layers in relation to doping.

2. Model

The extent of the wave functions in the plane of the layers should also be limited because of the finite lifetime of an electron in a given subband. Occupying a limited area, certain quantum states of an electron interact with a limited amount of impurities. Due to spatial fluctuations in the impurity concentration, there should be a fluctuation in the electron's eigen energy and, consequently, a broadening of spectral lines.

Let us quantify this phenomenon by determining the extent of the wave functions, i.e., the coherence length. We believe that due to the finite lifetime of the electrons in the τ subbands, the average coherence length of their wave functions in the plane of the layer is

$$L = \tau \, \bar{\nu}_x = \tau \, \sqrt{\frac{k_{\rm B}T}{m_c}},\tag{1}$$

where we use the root mean square projection of the thermalvelocity $\sqrt{\langle v_x^2 \rangle}$ as the root mean square projection.

The same expression for the coherence length is obtained when considering the energy structure of the levels, taking into account spectral broadening. The size of the region at which the energy gap between adjacent levels is equal to the broadening parameter $\gamma = \hbar/\tau$ is determined by the ratio

$$\frac{dE}{dk}\Delta k = \gamma,\tag{2}$$

where E and k are the energy and wave vector of the electron. Next, let us use the effective mass approximation $E = \hbar^2 k^2 / 2m_c$ and the sampling step for zero boundary

¹ Belarusian State University,

conditions $\Delta k = \pi/L$, and also consider states with an average energy close to thermal energy. For one degree of freedom $E = k_{\rm B}T/2$. After calculating $dE/dk = \hbar^2 k/m_c$ and substituting $\hbar k = \sqrt{m_c k_{\rm B}T}$, we obtain the expression (1).

The amount of impurities that enter the site $L \times L$ is determined by the Poisson distribution. The variance of this distribution is equal to the average number of impurities in the selected area, so that the RMS value of the fluctuation in the number of impurities is

$$\Delta N = \sqrt{N_{2d}L^2},\tag{3}$$

where N_{2d} is the layer concentration of doping.

The interaction of an electron with a charged impurity is described by a screened Coulomb potential

$$V(\mathbf{r}) = -\frac{e^2 \exp(-q_{\text{scr}}r)}{4\pi\varepsilon\varepsilon_0 r},\tag{4}$$

where $q_{\rm scr}=\sqrt{e^2N_{3d}/\varepsilon\varepsilon_0k_{\rm B}T}$ is the reverse screening length, ε is the permittivity, N_{3d} is the bulk doping concentration, T is the temperature.

Next, let's consider two cases. The first case is when the coherence length L is much longer than the screening length $1/q_{\rm scr}$. In this case, it can be assumed that the electronic state interacts only with impurities entering the site $L \times L$. The change in the energy of the state $\varphi_i(\mathbf{k},z)$ with the wave vector \mathbf{k} due to interaction with an impurity is described by the matrix element

$$V_{ii}(z_0) = \int \varphi_i^*(\mathbf{k}, z) V(z - z_0) \varphi_i(\mathbf{k}, z) dz.$$
 (5)

Here, the zero Fourier component of the Coulomb potential of a plane wave in the plane of the layer is

$$V(z) = -\frac{e^2}{2\varepsilon\varepsilon_0 q_{\rm scr} L^2} \exp(-q_{\rm scr}|z|). \tag{6}$$

Taking into account the expressions (3) and (5) the RMS fluctuation of the energy of the state with fluctuations in the number of impurities in the region limited by the coherence of the wave functions is

$$\sigma_i = \sqrt{N_{2d} L^2 \langle V_{ii}^2(z_0) \rangle}. \tag{7}$$

Here, the brackets indicate the averaging over the impurity position z_0 . When considering transitions between levels, we use the energy difference between the final and initial states for broadening:

$$\sigma_{fi} = \sqrt{N_{2d}L^2 \langle \left(V_{ff}(z_0) - V_{ii}(z_0)\right)^2 \rangle}.$$
 (8)

Taking into account the expression (6) heterogeneous broadening due to fluctuations in impurity concentration (8) is inversely proportional to the coherence length and directly proportional to the square root of the impurity concentration.

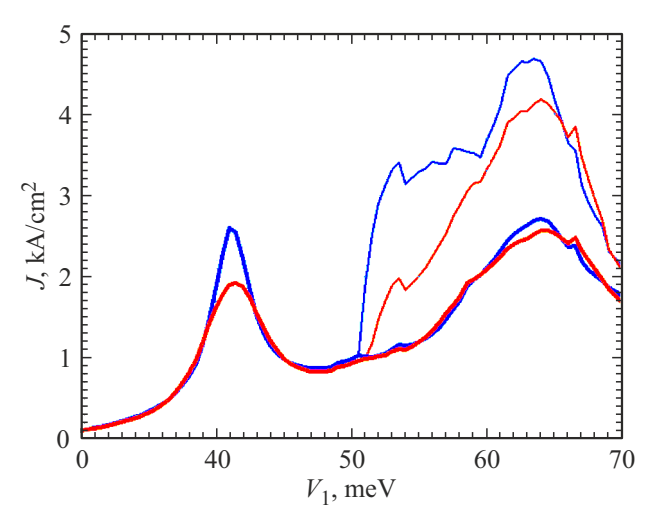


Figure 1. The dependence of current density on voltage on one cascade without taking into account (blue curve) and taking into account (red curve) the heterogeneous broadening of energy levels during fluctuations in doping concentration. Thin lines show the characteristics in the generation mode.

The second case is when the coherence length L is much smaller than the screening length $1/q_{\rm scr}$. In this case, the electronic state interacts with all neighboring impurities, not just those entering the site $L \times L$. In the domain of the existence of the wave function, the screened Coulomb potential(4) depending on the polar coordinate of ρ , it can be considered constant and taken as an integration sign. Then the interaction energy is calculated as

$$V_{ii}(\boldsymbol{\rho}, z_0) = \int \varphi_i(z) V(\boldsymbol{\rho}, z - z_0) \varphi_i(z) dz.$$
 (9)

Here, the radius vector \mathbf{r} is represented in polar coordinates as $\boldsymbol{\rho}$ and z. The RMS fluctuation of the energy of the state during the fluctuation of the impurity potential is

$$\sigma_i = \sqrt{N_d \left\langle \int V_{ii}^2(\boldsymbol{\rho}, z_0) d\boldsymbol{\rho} \right\rangle}.$$
 (10)

The integral in the expression (10) diverges in the limiting two-dimensional case. The expression for the RMS energy fluctuation for a bulk semiconductor would be

$$\sigma_{3d} = \frac{e^2}{\varepsilon \varepsilon_0} \sqrt{\frac{N_{3d}}{8\pi q_{\rm scr}}}.$$
 (11)

It should be noted that the considered heterogeneous broadening is described by the Poisson distribution, while the homogeneous broadening, determined by the finite lifetime of electrons in the subbands, has a Lorentzian form. If there are several impurities interacting with the coherent wave function, then the Poisson distribution is close to the normal distribution. Therefore, further in the calculations, the shape of the spectral lines was approximately described by the Voigt profile, which is obtained by convolving the

Lorentz and Gaussian form factors. The half-width of the spectral line for the heterogeneous broadening was determined from the ratio

$$\gamma = \sigma \sqrt{2 \ln 2}.\tag{12}$$

3. Calculation results

The structure of the quantum cascade laser 4 layers Al_{0.2}Ga_{0.8}As/GaAs with a period of 1.90/**16.46**/3.26/**7.99** nm was analyzed in this study [9]. Here, the wide and narrow quantum wells (QWs) are highlighted by bold font. The central part of the wide QW with a length of 3.38 nm is doped by donors to a concentration of $1.3 \cdot 10^{17} \, \text{cm}^{-3}$. The coordinate wave functions and the profile of the electrostatic potential were self-consistently determined by sequentially solving the Schrodinger equation in the three-band $\mathbf{k} \cdot \mathbf{p}$ approximation and the Poisson equation. The broadening of transition levels and rates took into account the processes of tunneling, scattering by optical phonons, ionized impurities, and roughness of heterogeneous boundaries. homogeneous broadening of the transition was considered to be equal to the average of the broadening of the initial and final states.

The screening length was 17.6 nm at a temperature of 77 K. For homogeneous broadening of levels of 2 meV, the coherence length is equal to 43 nm and is more than 2 times the screening length. Therefore, the ratio (8) was used to calculate the broadening. The average number of impurities per site $L \times L$ in one period is 0.85. The position of the impurity was averaged over 9 periods, and, accordingly, the number of impurities per site was increased by the same number of times. The RMS broadening in the approximation of a bulk semiconductor (11) is 5.4 meV. As the temperature increases, the values of homogeneous broadening increase in proportion to the scattering rate, and

the values of heterogeneous broadening (8) decrease due to an increase in the coherence length (1).

The calculated current-voltage curve is shown in Figure 1. The main current density maxima are observed near 42 and 63 mV. The first maximum corresponds to the resonant tunneling of the ground state I wide QW into the excited state 3 wide QW of the next cascade (Figure 2, a). The second maximum corresponds to the resonant tunneling of the ground state I of the wide QW into the ground state 2 of the neighboring narrow QW (Figure 2, b).

The magnitude of the heterogeneous broadening of the transition lines may exceed the values for the homogeneous broadening (Figure 3). For a given voltage across the cascade, the heterogeneous broadening increases with increasing diversity of the electron density of states in space. The transition 3-1' has the smallest broadening, for which the wave functions are in the same wide QW. The following are the extension parameters for transitions 1-2 and 2-3 between wave functions in neighboring wide and narrow quantum wells. The transition 1-3 has the greatest broadening, for which the wave functions are found at wide intervals through the period.

The current carrier transfer is limited by the resonant tunneling rate I-3 for the voltage of $42\,\mathrm{mV}$ across the cascade, since the probability of transitions 3-I' with the emission of optical phonons is great. The half-widths of the homogeneous and heterogeneous form factors were 1.4 and 2.1 meV, respectively. The half-width of the resulting form factor was $2.9\,\mathrm{meV} - 2\,\mathrm{times}$ the value of the homogeneous broadening. This reduced the probability of the transition and led to a partial smoothing of the first tunnel resonance (transition I-3) (see Figure 1). The low severity of the first tunnel resonance is in better agreement with experimental data [9]. The transfer of current carriers is limited by the transition rate 2-3 for the second resonant peak at $V_1=63\,\mathrm{meV}$. The half-widths of the homogeneous, heterogeneous, and resulting form factors were 2.1, 2.3 and

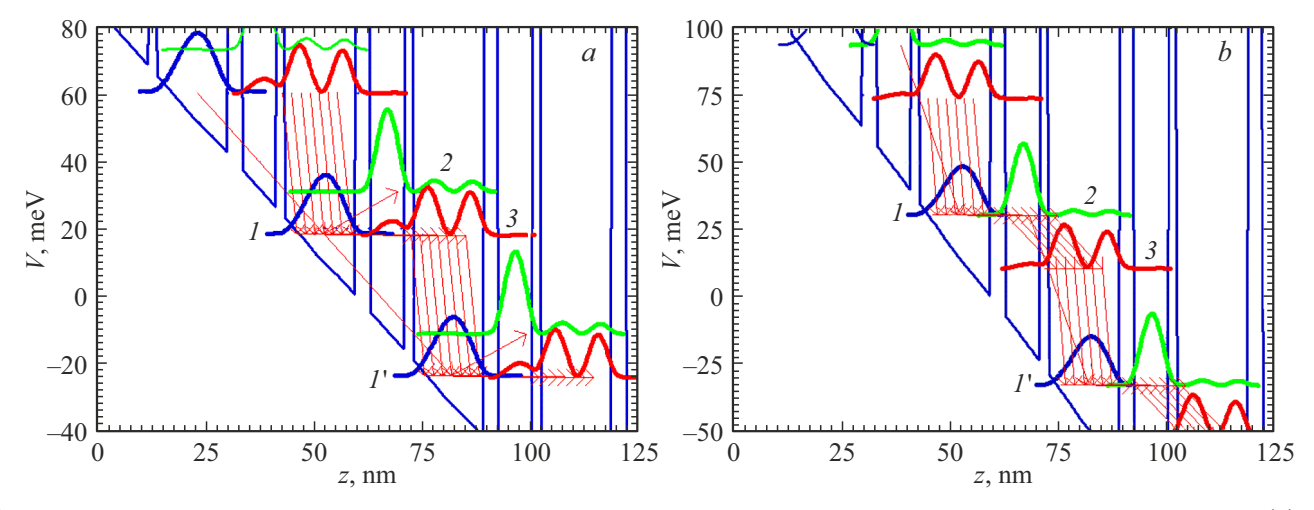


Figure 2. The profile of the bottom of the conduction band and the squares of the wave functions at cascade voltages of 42 (a) and 63 (b) mV. The arrows show the electron transfer.

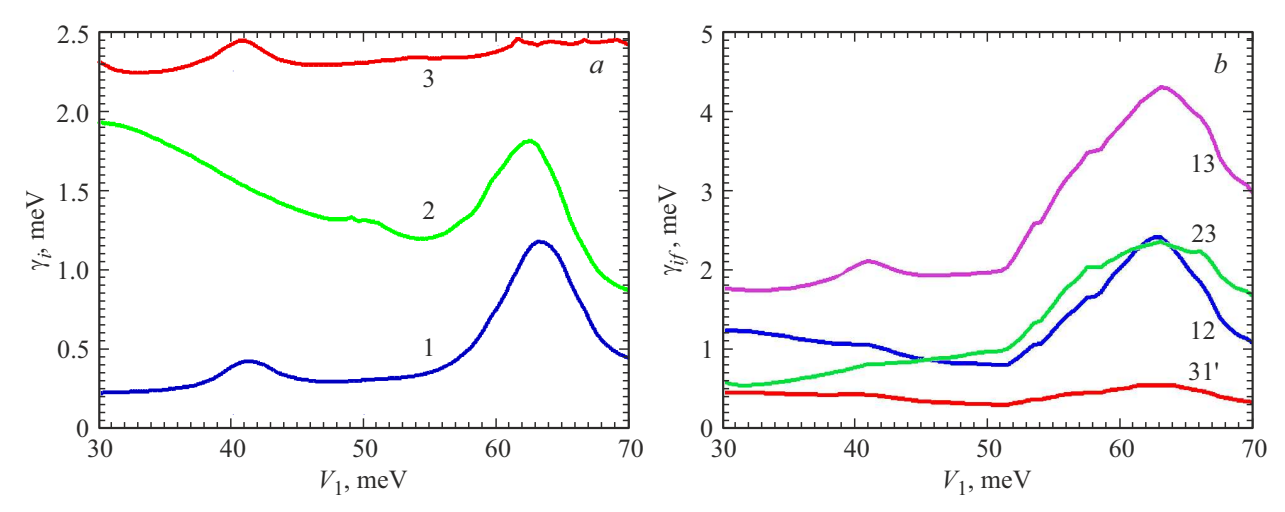


Figure 3. Dependence of the half-width of homogeneous broadening for levels 1, 2, 3 (a) and heterogeneous broadening for transitions 1-2, 2-3, 3-1' (b) from voltage on one stage.

 $3.6\,\mathrm{meV}$, respectively. However, due to the nonresonant nature of elastic scattering (detuning $\sim 16\,\mathrm{meV}$), the value of the Voigt form factor differs little from the value of the initial Lorentz form factor, and the current density, taking into account and without heterogeneous broadening, practically coincide (see Figure 1). For stimulated radiation, the transition 2-3 is resonant, therefore, heterogeneous broadening leads to a decrease in gain, a decrease in generation power, and a decrease in the corresponding current density (see Figure 1).

4. Conclusion

The authors analyzed heterogeneous broadening in quantum cascade laser heterostructures due to fluctuations in the concentration of impurities with a coherence length of wave functions exceeding the length of the Coulomb potential screening. The study showed that taking into account heterogeneous broadening leads to a decrease in the probability of resonant transitions and practically does not affect the probability of nonresonant transitions. The magnitude of the heterogeneous broadening turns out to be greater for wave functions spaced apart. It is found that for quantum cascade lasers with a period of two quantum wells, the value of the homogeneous broadening of the three basic levels, calculated taking into account the processes of tunneling, scattering by optical phonons, ionized impurities, and roughness of heterogeneous boundaries, is in the range of 0.3-2.5 meV, and the value of the heterogeneous broadening of the transition lines is in the range of 0.3-4.3 meV depending on the applied voltage.

Funding

The heterogeneous broadening of energy levels was calculated with the support of the Belarusian Republican Foundation for Fundamental Research, grant No. 23RNFM-064. Experimental data for the verification of the models

used were obtained with the financial support of the state task of SRC "Kurchatov Institute".

Conflict of interest

The authors declare that they have no conflict of interest.

References

- A. Khalatpour, M.Ch. Tam, S.J. Addamane, J. Reno, Z. Wasilewski, Q. Hu. Appl. Phys. Lett., 122, 161101 (2023).
- [2] X. Wang, C. Shen, T. Jiang, Z. Zhan, Q. Deng, W. Li, W. Wu, N. Yang, W. Chu, S. Duan. AIP Advances, 6, 075210 (2016).
- [3] Y. Jin, J.L. Reno, S. Kumar. Optica, 7, 708 (2020).
- [4] D.V. Ushakov, A.A. Afonenko, A.A. Dubinov, V.I. Gavrilenko, O.Yu. Volkov, N.V. Shchavruk, D.S. Ponomarev, R.A. Khabibullin. Kvant. elektron., 49 (10), 913 (2019). (in Russian).
- [5] R.A. Khabibullin, K.V. Maremyanin, D.S. Ponomarev, R.R. Galiev, A.A. Zaitsev, A.I. Danilov, I.S. Vasilevsky, A.N. Vinichenko, A.N. Klochkov, A.A. Afonenko, D.V. Ushakov, S.V. Morozov, V.I. Gavrilenko. FTP, 55 (11), 989 (2021). (in Russian).
- [6] T.A. Bagaev, M.A. Ladugin, A.A. Marmalyuk, A.I. Danilov, D.V. Ushakov, A.A. Afonenko, A.A. Zaitsev, K.V. Maremyanin, S.V. Morozov, V.I. Gavrilenko, R.R. Galiev, A.Yu. Pavlov, S.S. Pushkarev, D.S. Ponomarev, R.A. Khabibullin. Pisma ZhTF, 48 (10), 16 (2022). (in Russian).
- [7] D.V. Ushakov, A.A. Afonenko, R.A. Khabibullin, V.K. Kononenko, I.S. Manak. Izv. Nats. Akad. Nauk Belarusi. Ser. fiz.-mat. navuk, 58 (2), 237 (2022).
- [8] R.A. Khabibullin, D.V. Ushakov, A.A. Afonenko, A.Yu. Pavlov, R.R. Galiev, D.S. Ponomarev, A.P. Vasilyev, A.G. Kuzmenkov, N.A. Maleev, F.I. Zubov, M.V. Maksimov, D.A. Belov, A.V. Ikonnikov, D.I. Kuritsyn, R.Kh. Zhukavin, K.A. Kovalevsky, V.A. Anfertev, V.L. Vaks, A.V. Antonov, A.A. Dubinov, S.V. Morozov, V.I. Gavrilenko. J. Appl. Phys., 136 (19), 194504 (2024).
- [9] M. Bosco, M. Franckie, G. Scalari, M. Beck, A. Wacker, J. Faist. Appl. Phys. Lett., 115 (1), 010601 (2019).

Translated by A.Akhtyamov